

Proportional-Integral (PI) Compensator Design of Duty-Cycle-Controlled Buck LED Driver



T. Madhukar Reddy
 M.Tech-Power Electronics,
 Department of EEE,
 SRTIST Nalgonda, Telangana.



B. Ravi Kumar
 Associate Professor,
 Department of EEE,
 SRTIST Nalgonda, Telangana.

ABSTRACT

A discrete time-domain modelling and design for the duty-cycle-controlled buck light-emitting diode (LED) driver is presented in this paper. The discrete time-domain equation representing the buck LED driver is derived and linearized about the equilibrium state. Also the switching control law, the proportional integral (PI) compensator is used here as an example of the error amplifier, is linearized about the equilibrium state. The linearized buck LED driver and the control law are then combined to arrive at a linearized duty-cycle-controlled buck LED driver. The root locus method is employed to analyze the dynamic performance of the closed-loop system. Based on the modelling result, a practical design equation for the PI compensator is derived. Experimental results are presented to verify the validity of the proposed PI compensator design.

INTRODUCTION

Over the past few years, light-emitting diode (LED) technology has emerged as a promising technology for residential, automotive, decorative, and medical applications. This is mainly caused by the enhanced efficiency, energy savings and flexibility, and the long lifetime. Today, LEDs are available for various colours and they are suitable for white illumination. The luminous flux of LEDs is mostly determined by the LED forward current. Controlling the current accurately is a challenge when each LED has a large manufacturing tolerance in its forward voltage.

Therefore, the regulated constant current control is needed to achieve constant brightness of LEDs. Recently, many works, which include power factor correction methods, current sharing for LED strings, and thermal design, have been done for power LED applications.

Small-signal linearized modelling for the current regulated LED driver is of crucial importance in many applications not only for assessing stability and dynamic characteristics but for designing compensators. Numerous attempts have been made to characterize the switching converter system. The average concepts successfully used in the modelling of power converters.

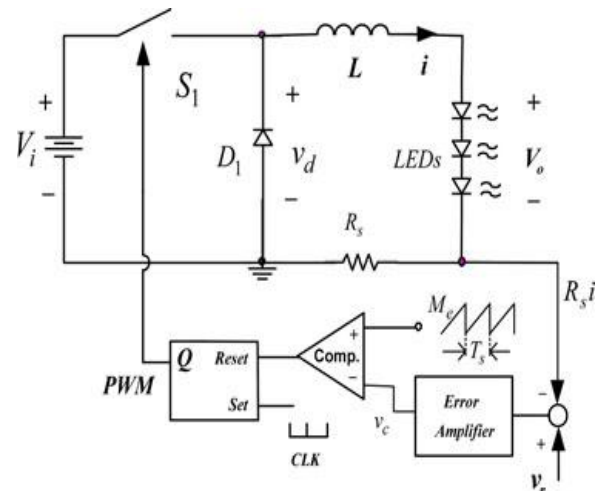


Fig.1 Duty-cycle-controlled buck LED driver with constant-frequency controller.

The low-frequency response can be well predicted by the average models. However, one common issue of the average models is that they cannot predict sub harmonic oscillations in current-mode control. Exact discrete-time model can accurately predict responses. This numerical technique is not useful to be used in practical design. In order to extend the validation of the average models to the high-frequency range, modified average models are proposed based on the results of discrete-time analysis and sampled-data analysis. All mentioned modelling approaches are related to voltage regulated converters. Very little work has been done in the area of modeling and control to improve dynamic performance of the current regulated LED driver.

In this paper, the systematic discrete time-domain approaches adapted to modelling and designing feedback compensator for the duty-cycle-controlled buck LED driver shown. Root-locus analysis is used to derive the stability boundaries and the practical design equation for selecting the optimum proportional-integral (PI) gains of the error amplifier. Experimental results are presented to confirm the validity of the proposed design method.

DESIGN GUIDELINES

Bode plots have been commonly used to assess the stability of the closed-loop system by finding the phase margin, but these plots cannot give information on the dynamic behavior of the individual state variables. On the other hand, root-locus analysis can provide the engineer with the stability and the transient performance of the individual state variables related to the location of the roots of the characteristic equation. To analyze the stability and dynamic characteristics of the closed-loop system, the eigenvalues of the system matrix misevaluated. The eigenvalues of A is the solutions of

$$|A - zI| = 0 \quad (14)$$

Where I is the identity matrix. The following root-locus analysis is performed for $R_s = 1$.

The root locus as a function of the P gain k_p for $k_{ni} = 0.2, D = 0.45$, and $Sr = 0.82$ is shown in Fig. 2. Corresponding pole locations between the s -plane and the z -plane are shown. The eigenvalues λ_1 and λ_2 in the z -plane are mapped to s_1 and s_2 in the s -plane, respectively. Unlike the peak current-controlled buck LED driver reported in, this duty cycle-controlled buck LED driver is unstable for $k_{ip} = 0$.

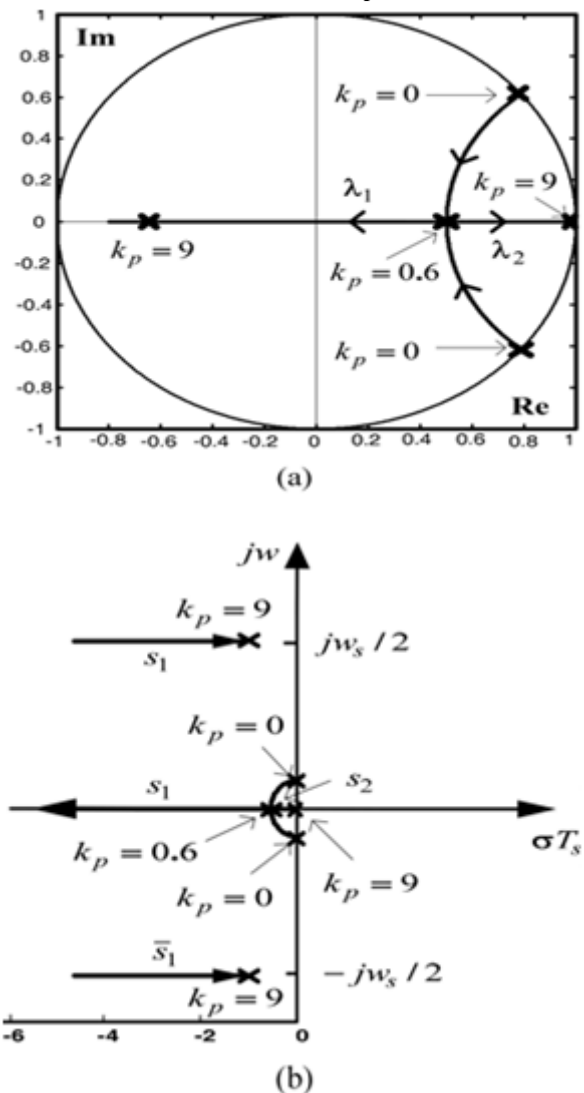


Fig. 2 Root locus as a function of the P gain k_p : (a) in the z -plane and (b) in the s -plane ($k_{ni} = 0.2, D = 0.45, Sr = 1.0D - 1 - D = 0.82$).

The Eigen value λ_1 is dominated by the inductor current state. The transient response of λ_1 after a disturbance is underdamped when k_p is between 0 and 0.6. At $k_p = 0.6$, the system response is critically

damped. And then, λ_1 moves toward the origin of the unit circle with increasing k_p , which means the inductor current becomes faster. When k_p is greater than 0.6, the transient response of the inductor current is over damped. Increasing k_p much further, the current response is under damped with a natural resonant frequency equal to $f_s/2$ due to the negative real value of λ_1 . On the other hand, the eigenvalue λ_2 is dominated by the capacitor voltage state of the error amplifier. The transient response of λ_2 is under damped when k_p is between 0 and 0.6 due to the two complex roots. Then, λ_2 moves toward the unit circle with increasing k_p , which means the capacitor voltage becomes slower. The capacitor voltage is over damped when k_p is greater than 0.6. The relationship between the s -plane poles and the z -plane poles is $z = e^{sTs}/s = \sigma \pm j\omega = e^{\sigma Ts} \pm wTs$.

The detailed information about the time response of the discrete system can be found in. The root locus as a function of the I gain k_{ni} for $k_p = 0.84, D = 0.4$, and $Sr = 1.0$ is shown in Fig. 5. When the I gain k_{ni} is increased from 0 to 0.27, the transient response is changed from over damped to critically damped, and the overall system

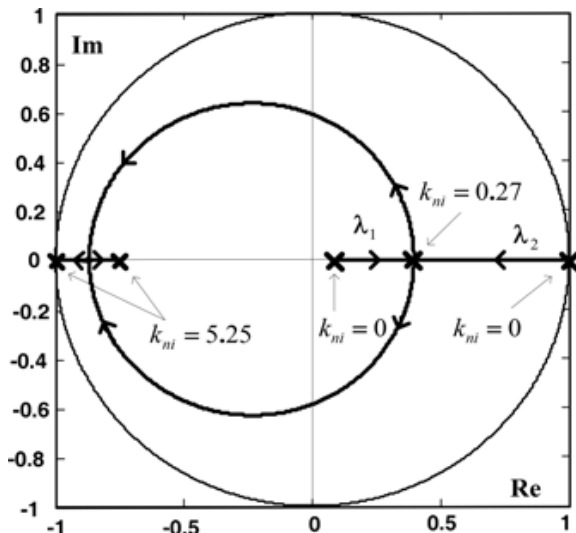
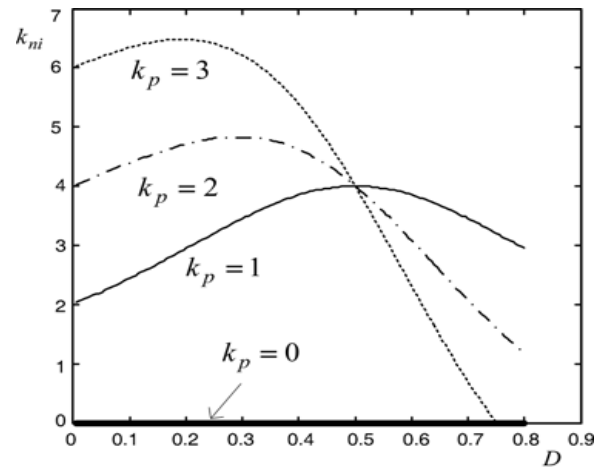
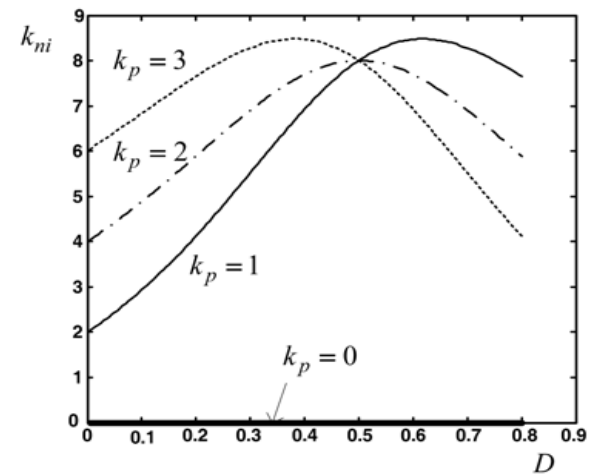


Fig. 3 Root locus as a function of the I gain k_{ni} ($k_p = 0.84, D = 0.4, Sr = 1.5D1 - D = 1.0$).



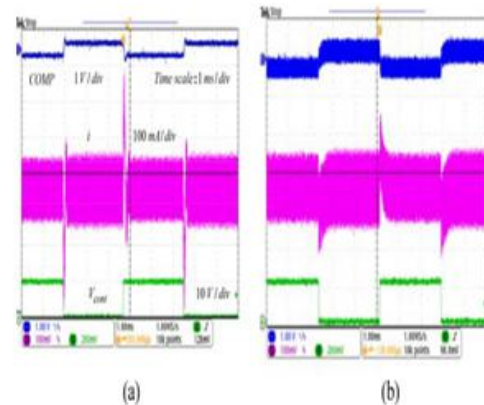
(a)



(b)

Fig. 4 Theoretical stability boundaries of k_{ni} as a function of D . (a) $Sr = 1.0D1 - D$. (b) $Sr = 2D1 - D$.

EXPERIMENTAL EVALUATION



(a)

(b)

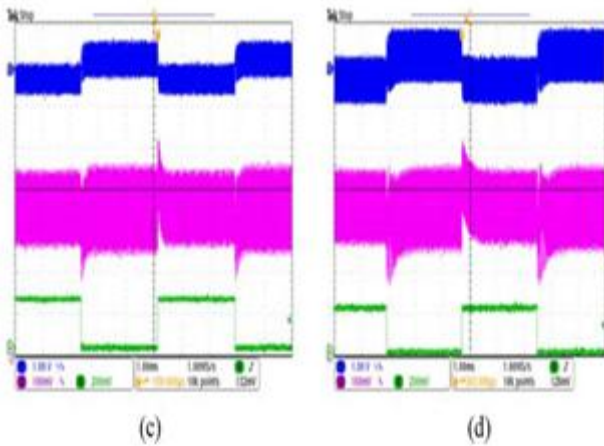


Fig. 5. Transient responses for step load change between 3 and 5 LEDs ($V_i=40$ V, $k_{ni}=0.2$, $R_2=12$ k, $C_1=10$ nF). (a) $k_p=0.1$ ($R_1=0.5$ k). (b) $k_p=0.84$ ($R_1=4.2$ k). (c) $k_p=1.3$ ($R_1=6.5$ k). (d) $k_p=2.0$ ($R_1=10$ k).

The constant switching frequency is 100 kHz. The normal operating range of D in the converter is between 0.2 and 0.6. In the experiment, the ramp peak-to-peak amplitude ΔV is $1.7/3 \approx 0.567$ V, which is generated with 13 of the oscillator peak-to-peak amplitude 1.7 V. The ramp slope M_{ei} is $\Delta V/T_s = 0.567 \times 100 \times 10^3$. The control IC is CS3842. S is IRF 840 and $D1$ is DSEI12-06A. Here, we use pure-white LEDs, Z-POWER w42182, which has a typical current of 350 mA. This LED forward voltage varies from 3.0 to 4.0 V, for a nominal of 3.25 V. The output voltage is approximately $(3.25 \text{ V} \times 5 \text{ LEDs in series})$

16.25 V. S_{ri} is

$$\frac{M_e}{(V_o R_s / L) k_{ni}} \frac{1}{k_{ni}} = \frac{0.567 \times 100 \times 10^3}{\{16.25 \times 1 / (430 \times 10^{-6})\} k_{ni}} \frac{1}{k_{ni}} = \frac{1.5}{k_{ni}}$$

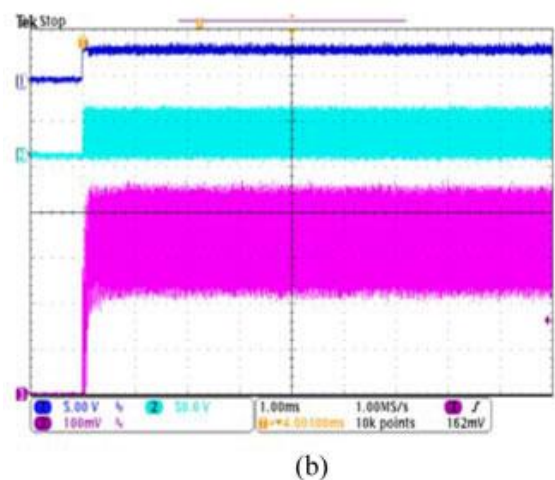
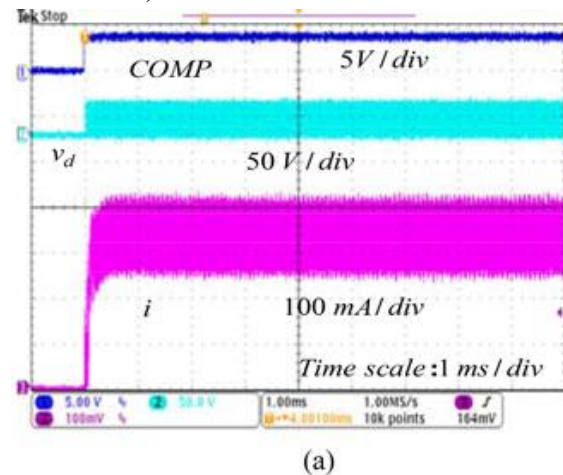
for $R_s=1\Omega$, and S_{ri} is $1.5D/1-D$. Setting $k_{ni}=0.2$, S_{ri} is

$$7.5, \frac{k_p}{k_{ni}} \text{ is } (1-2D) + \sqrt{2(1-D)(S_{ri} \frac{2D}{1-D} - D)} = 4.0$$

for the maximum $D=0.6$. The designed k_p is selected to be 0.84, which is slightly greater than 0.8 for $k_{ni}=0.2$. The integral gain $k_i = k_{ni}/T_s = 0.2 \times 100 \times 10^3 = 20000$. The PI gains are distributed throughout the feedback path between the current sense and the comparator input. The gain of LM324 is $1.2k + 7.4k/1.2k = 7.16$. The function of LM 324 is converting the

sensed R_{sio} to the internal reference voltage of the error amplifier. The average value of the output voltage of LM 324 is equal to the reference voltage of the error amplifier input, which is 2.5 V in the datasheet [29]. From the datasheet, the internal gain between COMP and the comparator input is 13. The overall proportional gain k_p and integral gain k_i are $7.16/3 \times R_1/R_2$ and $7.16/3 \times 1/R_2 C_1$, respectively. For the designed integral gain $k_i=20000$, the values of R_2 and C_1 are chosen to be 12 k and 0.01 μF . For the designed proportional gain $k_p=0.84$, the value of R_1 is chosen to be 4.2 k.

With five LEDs connected in series, which provides a typical loading voltage of approximately $(3.25 \text{ V} \times 5 \text{ LEDs in series})$



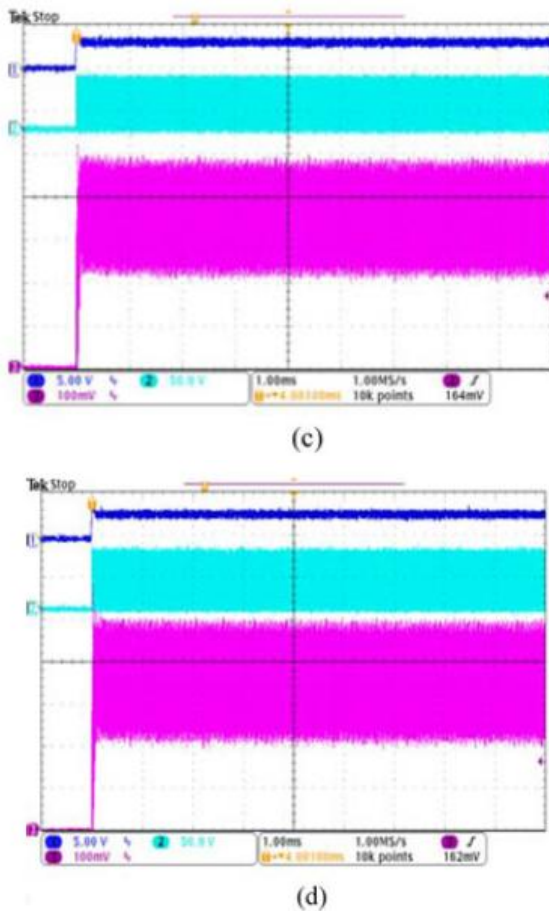


Fig.6 Start-up transient responses with increasing the input voltage ($V_o \approx 16.25$ V, $k_p = 0.84$, $k_{ni} = 0.2$).
 (a) $V_i = 30$ V ($S_r \approx 1.77$). (b) $V_i = 50$ V ($S_r \approx 0.72$) (c) $V_i = 60$ V ($S_r \approx 0.56$) (d) $V_i = 70$ V ($S_r \approx 0.45$).

16.25 V, the LED currents are measured for start-up transience with increasing P gain as shown. As the P gain increases from $k_p = 0.1$ to $k_p = 1.3$, the transient response of the LED current changes from under damped to over damped response, and then, to a slower and poor transient response due to the slower error amplifier state for $k_p = 2.0$. This experimental response shows a good agreement with the prediction of the root-locus analysis.

CONCLUSION

A discrete time-domain modelling and analysis for the duty cycle-controlled buck LED driver has been presented. The discrete time-domain equation that represents the static and dynamic behaviour of the

buck converter is derived and linearized about the equilibrium state of the buck converter. Also the duty cycle control law is linearized about the equilibrium state. The linearized buck converter and the linearized duty cycle control law are then combined to arrive at a linearized duty-cycle controlled LED driver.

The PI compensator is used as an example of the error amplifier. Increasing P gain from zero, the transient response of the inductor current state changes from under damped to overdamped, and then, to under damped with natural resonant frequency equal to half of the switching frequency. The duty-cycle controlled buck LED driver is always unstable for $k_p = 0$. The stable integral gain range is very wide for a given P gain. Impractical design, it is desirable that the transient response of the inductor current should be critically damped or slightly overdamped to avoid an oscillatory LED current. Based on this concept, the PI gains can be determined at the maximum D_{in} in the range of operating region. Therefore, for a good transient response, the P gain k_p slightly greater than or equal to $k_{ni} \{ (1 - 2D_{max}) + \sqrt{2(1 - D_{max})(S_r / 2D_{max} - 1 - D_{max})} \}$ can be selected. Selecting the PI gains of the error amplifier according to this practical design equation is very easy and useful for the design engineer. Experimental results are presented to confirm the validity of the proposed PI compensator design.

REFERENCES

- [1] D. G. Lamar, M. Arias, A. Rodriguez, A. Fernandez, M. M. Hernando, and J. Sebastian, "Design-oriented analysis and performance evaluation of a low-cost high-brightness LED driver based on flyback power factor corrector," *IEEE Trans. Ind. Electron.*, vol. 60, no. 7, pp. 2614–2626, Jul. 2013.
- [2] Seoul Semiconductor Co., LTD. (2009). Z-power LED series—technical datasheet for X4218X. [Online]. Available: <http://www.seoulsemicon.com/kr/html/main/>

- [3] C. B. Park, B. H. Choi, J. P. Cheon, and C. T. Rim, "Robust active LED driver with high power factor and low total harmonic distortion compatible with a rapid-start ballast," *J. Power Electron.*, vol. 14, no. 2, pp. 226–236, Mar. 2014.
- [4] H. H. Chou, Y. S. Hwang, and J. J. Chen, "An adaptive output current estimation circuit for a primary-side controlled LED driver," *IEEE Trans. Power Electron.*, vol. 28, no. 10, pp. 4811–4819, Oct. 2013.
- [5] Q. Hu and R. Zane, "Minimizing required energy storage in off-line LED drivers based on series-input converter modules," *IEEE Trans. Power Electron.*, vol. 26, no. 10, pp. 2887–2895, Oct. 2011.
- [6] W. Chen and S. Y. R. Hui, "Elimination of an electrolytic capacitor in AC/DC light-emitting diode (LED) driver with high input power factor and constant output current," *IEEE Trans. Power Electron.*, vol. 27, no. 27, pp. 1598–1607, Mar. 2012.
- [7] Y. X. Qin, H. S. H. Chung, D. Y. Lin, and S. Y. R. Hui, "Current source ballast for high power lighting emitting diodes without electrolytic capacitor," in *Proc. IEEE Ind. Electron. Conf.*, 2008, pp. 1968–1973.
- [8] J. M. Alonso, J. V. V. V. Vaquero, G. Martinez, and R. Osorio, "Analysis and design of the integrated double buck-boost converter as a high-power factor driver for power-LED lamps," *IEEE Trans. Ind. Electron.*, vol. 59, no. 4, pp. 1689–1697, Apr. 2012.
- [9] F. Zhang, J. Ni, and Y. Yu, "High power factor AC-DC LED driver with film capacitors," *IEEE Trans. Power Electron.*, vol. 28, no. 10, pp. 4831–4840, Oct. 2013.
- [10] Q. Luo, S. Zhi, C. Zou, W. Lu, and L. Zhou, "An LED driver with dynamic high-frequency sinusoidal bus voltage regulation for multistring applications," *IEEE Trans. Power Electron.*, vol. 29, no. 1, pp. 491–500, Jan. 2014.
- [11] X. Wu, C. Hu, J. Zhang, and C. Zhao, "Series-parallel autoregulated charge-balancing rectifier for multioutput light-emitting diode driver," *IEEE Trans. Ind. Electron.*, vol. 61, no. 3, pp. 1262–1268, Mar. 2014.
- [12] X. Wu, Z. Wang, and J. Zhang, "Design considerations for dual-output quasi-resonant flyback LED driver with current-sharing transformer," *IEEE Trans. Power Electron.*, vol. 28, no. 10, pp. 4820–4830, Oct. 2013.
- [13] K. H. Loo, Y. M. Lai, and C. K. Tse, "Design and analysis of LCC resonant network for quasi-lossless current balancing in multistring AC LED array," *IEEE Trans. Power Electron.*, vol. 28, no. 2, pp. 1047–1059, Feb. 2013.
- [14] J. Patterson and R. Jane, "Series input modular architecture for driving multiple LEDs," in *Proc. IEEE Power Electron. Spec. Conf.*, Athens, Greece, Jun. 2008, pp. 2650–2656.
- [15] S. Y. R. Hui and Y. X. Qin, "A general photo-electro-thermal theory for light emitting diode (LED) systems," *IEEE Trans. Power Electron.*, vol. 24, no. 8, pp. 1967–1976, Aug. 2009.
- [16] R. D. Middlebrook, "Modeling current-programmed buck and boost regulators," *IEEE Trans. Power Electron.*, vol. 4, no. 1, pp. 36–52, Jan. 1989.
- [17] G. K. Schoneman and D. M. Mitchell, "Output impedance considerations for switching regulators with current-injected control," *IEEE Trans. Power Electron.*, vol. 4, no. 1, pp. 25–35, Jan. 1989.
- [18] F. C. Lee, R. P. Iwens, Y. Yu, and J. E. Triner, "Generalized computer-aided discrete-time modeling and analysis of dc-dc converters," *IEEE Trans. Ind. Electron. Contr. Instrum.*, vol. IECI-26, no. 2, pp. 58–69, May 1979.



[19] R. B. Ridley, "A new, continuous-time model for current-mode control," IEEE Trans. Power Electron., vol. 6, no. 2, pp. 271–280, Apr. 1991.

[20] F. D. Tan and R. D. Middlebrook, "A unified model for current-programmed converters," IEEE Trans. Power Electron., vol. 10, no. 4, pp. 397–408, Jul. 1995.